PHYSICAL REVIEW D **87,** 034504 (2013)

Color fields of the static pentaquark system computed in SU(3) lattice QCD

Nuno Cardoso* and Pedro Bicudo†

Departamento de Física, Instituto Superior Técnico, CFTP, Universidade Técnica de Lisboa, Avenida Rovisco Pais, 1049-001 Lisbon, Portugal

(Received 7 September 2012; published 11 February 2013)

We compute the color fields of SU(3) lattice QCD created by static pentaquark systems, in a $24^3 \times 48$ lattice at $\beta = 6.2$ corresponding to a lattice spacing $a = 0.07261(85)$ fm. We find that the pentaquark color fields are well described by a multi-Y-type shaped flux tube. The flux tube junction points are compatible with Fermat-Steiner points minimizing the total flux tube length. We also compare the pentaquark flux tube profile with the diquark-diantiquark central flux tube profile in the tetraquark and the quark-antiquark fundamental flux tube profile in the meson, and they match, thus showing that the pentaquark flux tubes are composed of fundamental flux tubes.

DOI: 10.1103/PhysRevD.87.034504 PACS numbers: 12.38.Gc

I. INTRODUCTION

Here we study the color field flux tubes produced by static pentaquarks in SU(3) lattice QCD. Unlike the color fields of simpler few-body systems, say mesons, baryons, and hybrids, [1–5], the pentaquark fields have not been previously studied in lattice QCD. This study is relevant both for the solution of theoretical problems and for the development of phenomenological models of QCD.

Quark confinement remains one of the main open theoretical problems of particle physics. In lattice QCD, flux tubes composed of color-electric and color-magnetic fields have been observed and this constitutes a very important clue for the understanding of quark confinement. Since the onset of QCD with its asymptotic freedom and infrared slavery, it is well known that confinement is due to the gluon fields and suppressed by the quark fields. It is thus important to measure the different possible flux tubes of pure gauge lattice QCD, to provide data for any theoretical attempt to solve the QCD confinement problem.

Moreover, in what concerns phenomenology, the study of the color fields in a pentaquark is important to discriminate between different multiquark Hamiltonian models, quark models with two-body interactions only [6] as in the original quark model, from the string flip-flop model with a multibody potential [7]. In the string flip-flop model, the color charges are connected by strings disposed geometrically in order to minimize the total string length. The strings constitute the limit of very thin elementary flux tubes. An elementary or fundamental flux tube is the flux tube connecting the quark and antiquark of a meson, where the quark is in the triplet or fundamental representation of QCD. For instance in the two quark two antiquark system, depending on the position of these color charges, the minimal string may be a two-meson string, or a tetraquark string, shaped like a double-Y flux tube, as in Fig. 1, composed of five linear fundamental flux tubes meeting in two Fermat-Steiner points [8–10]. A Fermat, or Steiner, point is defined as a junction minimizing the total length of strings, where linear individual strings join at 120° angles. When the positions of the color charges change, the potential may thus flip from one four-body potential to a pair of two-body potentials and flop back again. Notice the flip-flop potential, compatible with the confining component of the flux tubes explored here, lead to tetraquark bound states, below the strong decay threshold to pairs of mesons [8,11–13]. Recent investigations found that, even above the strong decay threshold, the presence of a centrifugal barrier in high angular momentum multiquarks may increase the stability of the system [7,14]. The multiquark Hamiltonians are important to understand not only the

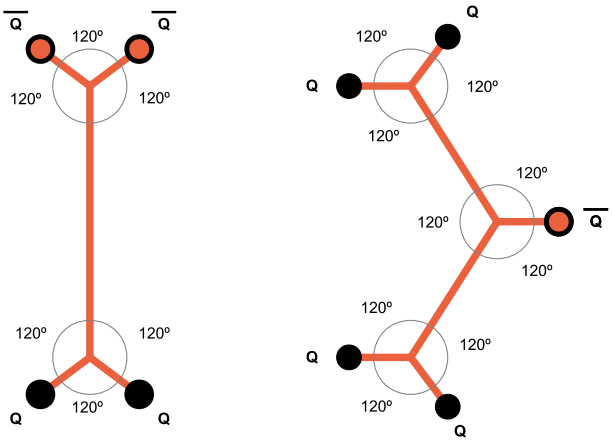

FIG. 1 (color online). In the string flip-flop model, thin elementary flux tubes similar to strings connect the color charges in order to minimize the total length of the strings. Whenever geometrically possible, three elementary flux tubes meet in a Fermat-Steiner point at an angle of $\alpha = 120°$. Here we depict planar examples of tetraquark and pentaquark flux tubes.

*nuno.cardoso@ist.utl.pt
†bicudo@ist.utl.pt

elusive multiquark hadrons, but also high density QCD where many quarks may overlap.

Experimentally, multiquark exotic hadrons have been searched for many years because as soon as the quarks were proposed in the sixties to classify the meson and baryon resonances, and the quark model was proposed in the seventies [15], it became clear that systems with more than three quarks could also possibly exist. One of the main problems of hadronic physics is thus to determine whether multiquark resonances exist or not, and whether the possible multiquark resonances are narrow or wide.

The simplest multiquark system is the tetraquark, and it was already proposed by Jaffe in the 1970s [16] as a bound state formed by two quarks and two antiquarks. Presently some observed resonances are tetraquark candidates. Very recently the Belle Collaboration made the tantalizing observation [17], in five different Υ (5S) decay channels of two new charged bottomonium resonances Z_b with masses of 10610 MeV$/c^2$ and 10650 MeV$/c^2$ and narrow widths of the order or 15 MeV. Since all standard bottomonia are neutrally charged, these two new resonances have a flavor only compatible with $b\bar{b}u\bar{d}$ tetraquarks. In 2003, the X(3872) observed by the Belle Collaboration [18,19] was suggested as a tetraquark candidate by Maiani *et al.* [20]. In 2004, the D_{sJ} (2632) state seen in Fermilab's SELEX [21,22] was suggested as a possible tetraquark candidate. In 2009, Fermilab announced the discovery of Y(4140), which may also be a tetraquark [23]. There are as well indications that the Y(4660) could be a tetraquark state [24]. The Υ (5S) bottomonium has also been recently suggested to be a tetraquark resonance [25]. However, a better understanding of tetraquarks is necessary to confirm or disprove the X, Y, Z, and possibly also other light resonance candidates as tetraquark states.

The pentaquark is the next in the multiquark hadron series. Pentaquark hadrons were already proposed in the 1980s by Manohar [26] and Chemtob [27], inspired by extensions of the Skyrme model. In the 2000s a burst of interest was sparkled by a discovery claim of the Θ pentaquark by Nakano *et al.* [28]. This led to many experimental and lattice QCD studies of pentaquarks, together with hundreds of theoretical estimations of the Θ properties. However, the resonance Θ ended up by not being confirmed by the scientific community [29,30]. The many hundreds of publications on the subject, with disparate conclusions, show that the Θ pentaquark was beyond the scope of the scientific techniques utilized in the 2000s.

The multiquark hadrons are thus very elusive systems, much harder to observe experimentally, to understand in models, and to simulate in lattice QCD than the conventional mesons and baryons. Nevertheless, inasmuch as the understanding of confinement, the existence/nonexistence of multiquark hadrons remains an important problem in QCD, to be further explored in the future PANDA experiment at GSI.

It is thus important to proceed with the well-defined program of understanding the static potentials and flux tubes of multiquarks in quenched lattice QCD.

In the past years, the static tetraquark potential has been studied in lattice QCD computations [31–34]. The authors concluded that when the quark-quark are well separated from the antiquark-antiquark, the tetraquark potential is consistent with one gluon exchange Coulomb potentials plus a four-body confining potential, suggesting the formation of a double-Y flux tube, typical of the four-body potential of the string flip-flop model as in Fig. 1, composed of five linear fundamental flux tubes meeting in two Fermat-Steiner points [8–10]. This flux tube geometry was confirmed by lattice QCD studies of the flux tubes produced by a static tetraquark system [35,36]. In what concerns the pentaquark, static potentials have already been explored in a geometry with the antiquark situated in the center of the four quarks [32,37], also consistent with a string flip-flop model, in this case with only six fundamental flux tubes and two Fermat-Steiner points.

Here we proceed with the flux tube research program, studying the flux tubes of static pentaquarks in pure gauge SU(3) lattice QCD. In Sec. II we detail the framework we set to measure the flux tubes. We also extend the geometries explored in the static potential studies. In Sec. III we expose our results and conclude.

II. SIMULATING THE PENTAQUARK FLUX TUBES IN LATTICE QCD

The static potential for the pentaquark was already studied in the lattice QCD by Refs. [32,37,38] utilizing generalized Wilson loops. Here we use similar Wilson loops to place a static system of four quarks and one antiquark in the lattice, in four different geometries. Moreover, we measure the color-electric and color-magnetic fields produced by the static charges.

The Wilson loop operator for the pentaquark system is defined in a gauge-invariant way, as illustrated in Fig. 2, by

$$W_{5Q} = \frac{1}{3!}\epsilon^{ijk}\epsilon^{i'j'k'}M^{ii'}(R_3R_{12}R_4)^{jj'}(L_3L_{12}L_4)^{kk'}, \quad (1)$$

where

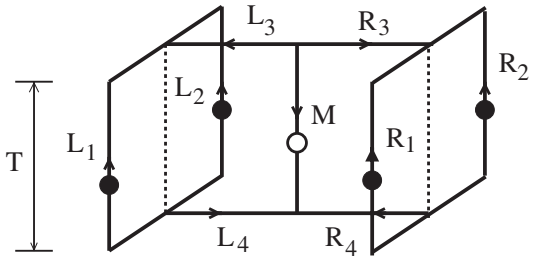

FIG. 2. Pentaquark Wilson loop as defined by Okiharu *et al.* [37,38]. Here we extend this Wilson loop with different paths L_i and R_i for the quarks and M_i for the antiquark.

$$R_{12}^{i'i} = \frac{1}{2}\epsilon^{ijk}\epsilon^{i'j'k'}R_1^{jj'}R_2^{kk'}, \qquad L_{12}^{i'i} = \frac{1}{2}\epsilon^{ijk}\epsilon^{i'j'k'}L_1^{jj'}L_2^{kk'}. \tag{2}$$

The projection in the spatial dimensions of our four different Wilson loop geometries for the static pentaquark is illustrated in Fig. 3. The distances of the geometries are quantified in Table I. The labeling of the geometries together with the number of lattice configurations used in this work are also shown in Table I.

We compute the color-electric and the color-magnetic fields, by using the correlators of the plaquettes $P_{\mu\nu}$ and the Wilson loop W_{5Q}. We define the plaquettes as $P_{\mu\nu} = 1 - \frac{1}{3}\,\mathrm{Tr}[U_\mu(\mathbf{s})U_\nu(\mathbf{s}+\boldsymbol{\mu})U_\mu^\dagger(\mathbf{s}+\boldsymbol{\nu})U_\nu^\dagger(\mathbf{s})]$.

With this definition, the chromofields are given by

$$\langle E_i^2\rangle = \langle P_{0i}\rangle - \frac{\langle W_{5Q}P_{0i}\rangle}{\langle W_{5Q}\rangle}, \tag{3}$$

$$\langle B_i^2\rangle = \frac{\langle W_{5Q}P_{jk}\rangle}{\langle W_{5Q}\rangle} - \langle P_{jk}\rangle, \tag{4}$$

with the indices j and k complementing index i. The Lagrangian and energy densities are given by $\mathcal{L} = \frac{1}{2}(E^2 - B^2)$ and $\mathcal{H} = \frac{1}{2}(E^2 + B^2)$.

To compute the static field expectation value, we plot the expectation value $\langle E_i^2(\mathbf{r})\rangle$ or $\langle B_i^2(\mathbf{r})\rangle$ as a function of the temporal extension T of the Wilson loop. At sufficiently large T, the ground state corresponding to the studied quantum numbers dominates, and the expectation value tends to a horizontal plateau. In order to improve the signal

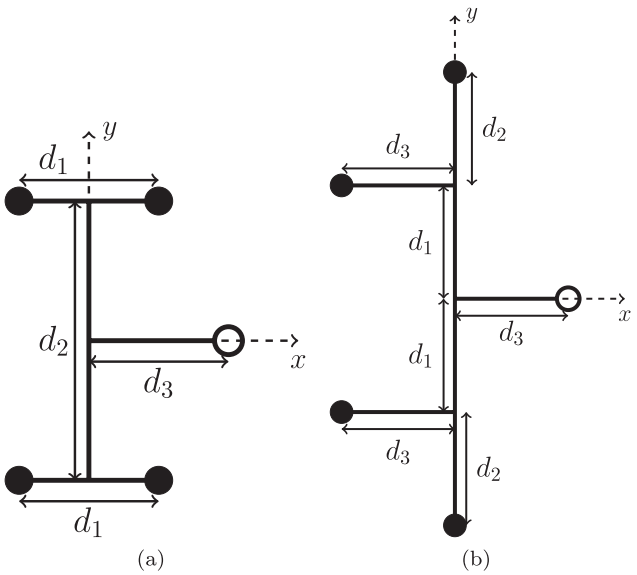

FIG. 3. Projection in the spatial dimensions of the different Wilson loop geometries for the static pentaquark studied in this work. The solid dots correspond to the quarks positions and the open dots to the antiquarks. The solid lines correspond to the spacelike Wilson paths.

TABLE I. Pentaquark geometries studied and number of lattice configurations used in this work. The geometry type is outlined in Fig. 3. The column Id corresponds to the numbering used in the text.

Id	Geometry type	d_1	d_2	d_3	# configurations
(i)	Figure 3(a)	8	8	0	551
(ii)	Figure 3(a)	8	8	6	549
(iii)	Figure 3(b)	4	4	8	544
(iv)	Figure 3(b)	6	4	8	1121

to noise ratio of the Wilson loop, we use 50 iterations of APE smearing with $w = 0.2$ (as in Refs. [4,35]) in the spatial directions and one iteration of hypercubic blocking in the temporal direction, [39], with $\alpha_1 = 0.75$, $\alpha_2 = 0.6$, and $\alpha_3 = 0.3$. Note that these two procedures are only applied to the Wilson loop, not to the plaquette.

To check if the pentaquark flux tube produces a clear signal, we study the χ^2/dof of our pentaquark T plateaux. Alexandrou *et al.* [32] compared the pentaquark potential and the sum of the baryonic and mesonic potentials and found that, when the separation between the two diquarks becomes larger than the internal diquark distance, the system is a genuine pentaquark state. But, surprisingly, the event at some of the distances illustrated in Fig. 4, where the string flip-flop potential would favor the meson-baryon flux tube, with a lower energy than the pentaquark flux tube, we find T plateaux with a good χ^2/dof. This shows that the mixing between the pentaquark flux tube and the meson-baryon flux tube is small, and this allows the study of clear pentaquark flux tubes even at relatively large diquark distances. The overlap of the two different color wave functions of the five quarks (antitriplet-antitriplet-antitriplet, and singlet-singlet) is too large to account for the small mixing we observe. We interpret this small mixing occurs because the pentaquark and the meson-baryon flux tubes have a very small overlap since they extend in different regions of space. Possibly, this could be clarified with the variational method of Cardoso *et al.* [36], used to study the flux tube recombination in two quarks and antiquarks.

To compute the fields, we fit the horizontal plateaux obtained for each point $\mathbf{r}$ determined by the plaquette position, but we consider $z = 0$ for simplicity. We finally compute the error bars of the fields with the jackknife method.

We compute the Fermat-Steiner points with the iterative method of Bicudo *et al.* [9]. We have five quarks (antiquarks) with the label i and three Fermat-Steiner points with label $a = I, II, III$,

$$\mathbf{r}_i = (x_i, y_i, z_i), \qquad \mathbf{r}_a = (x_a, y_a, z_a),$$
$$r_{ia} = \sqrt{(x_a - x_i)^2 + (y_a - y_i)^2 + (z_a - z_i)^2}. \tag{5}$$

To minimize the total length of the strings,

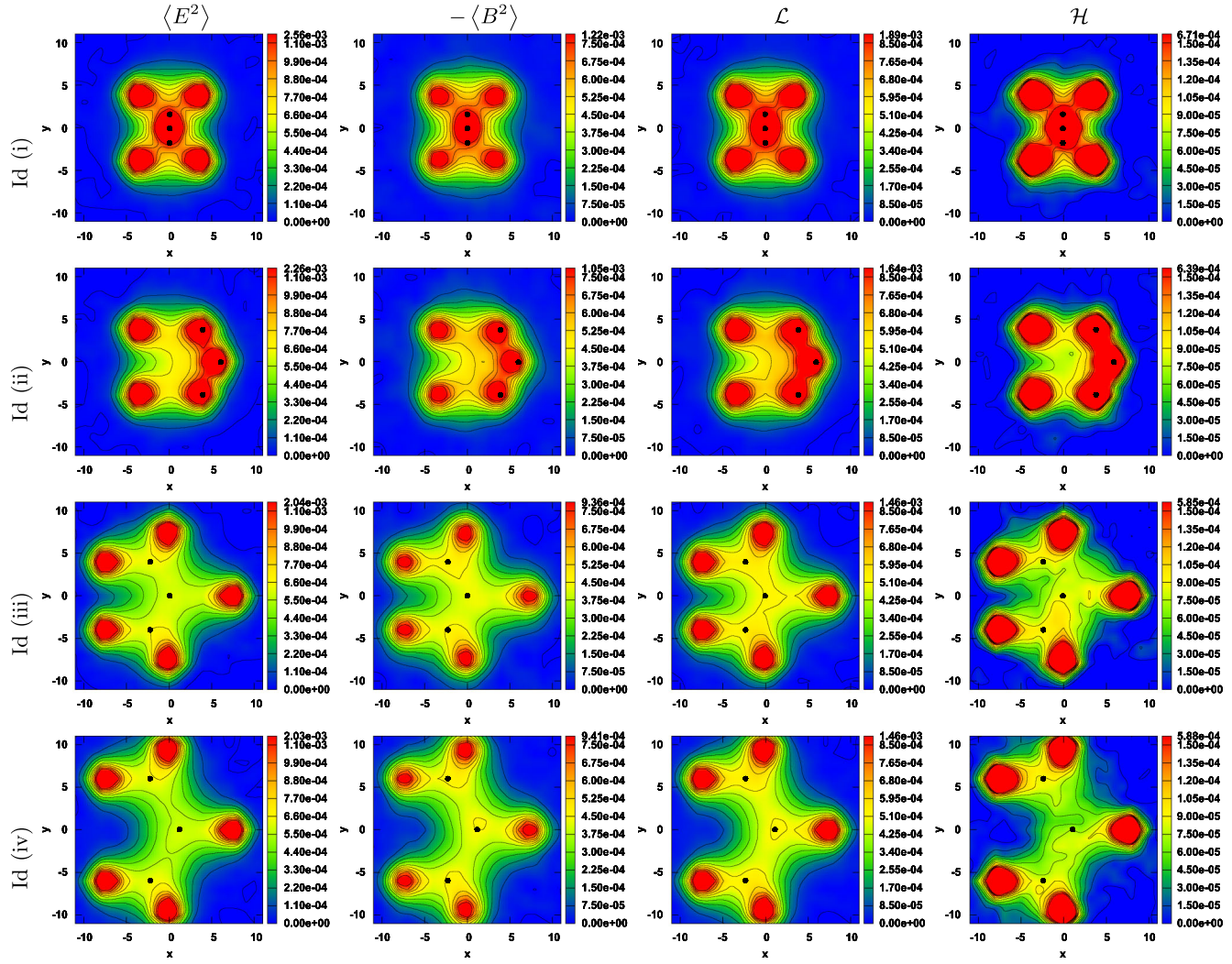

FIG. 4 (color online). Density plots of the chromoelectric and chromomagnetic fields and Lagrangian and energy densities for the geometries defined in Table I. The black dot points correspond to the Fermat-Steiner points, Table II. The results are presented in lattice spacing units.

$$d = r_{1\,I} + r_{2\,I} + r_{3\,II} + r_{4\,II} + r_{\bar{5}\,III} + r_{I\,III} + r_{II\,III}, \tag{6}$$

we only need to solve one nonlinear vector equation per Fermat-Steiner point,

$$\mathbf{r}_I = \frac{\frac{\mathbf{r}_1}{r_{1\,I}} + \frac{\mathbf{r}_2}{r_{2\,I}} + \frac{\mathbf{r}_{III}}{r_{III\,I}}}{\frac{1}{r_{1\,I}} + \frac{1}{r_{2\,I}} + \frac{1}{r_{III\,I}}}, \qquad \mathbf{r}_{II} = \frac{\frac{\mathbf{r}_3}{r_{3\,II}} + \frac{\mathbf{r}_4}{r_{4\,II}} + \frac{\mathbf{r}_{III}}{r_{III\,II}}}{\frac{1}{r_{3\,II}} + \frac{1}{r_{4\,II}} + \frac{1}{r_{III\,II}}},$$
$$\mathbf{r}_{III} = \frac{\frac{\mathbf{r}_I}{r_{I\,III}} + \frac{\mathbf{r}_{II}}{r_{II\,III}} + \frac{\mathbf{r}_{\bar{5}}}{r_{\bar{5}\,III}}}{\frac{1}{r_{I\,III}} + \frac{1}{r_{II\,III}} + \frac{1}{r_{\bar{5}\,III}}}. \tag{7}$$

III. RESULTS AND CONCLUSION

We remark that the signal is clear only if the paths considered in the Wilson loop overlap the flux tube. Thus, we consider geometries for the Wilson loop where the paths are just some lattice spacings distant from the expected string position in the string flip-flop model. We consider the four different Wilson loop geometries, detailed in Fig. 3 and in Table I. We only utilize planar geometries for the color sources, in order to produce clearer pictures of the fields. The results for the color field densities are presented only for the xy plane since the color sources are in this plane and the results with $z \neq 0$ are less interesting for this study. Then with color field densities as a function of x and y we produce density plots and three-dimensional plots.

To produce the results presented in this work, we utilize quenched configurations in a $24^3 \times 48$ lattice at $\beta = 6.2$. The number of configurations used is described in Table I. We present our results in lattice spacing units of a, with $a = 0.07261(85)$ fm or $a^{-1} = 2718 \pm 32$ MeV. We generate our configurations in NVIDIA GPUs of the FERMI series (480, 580 and Tesla C2070) with a SU(3) CUDA code upgraded from our SU(2) combination of

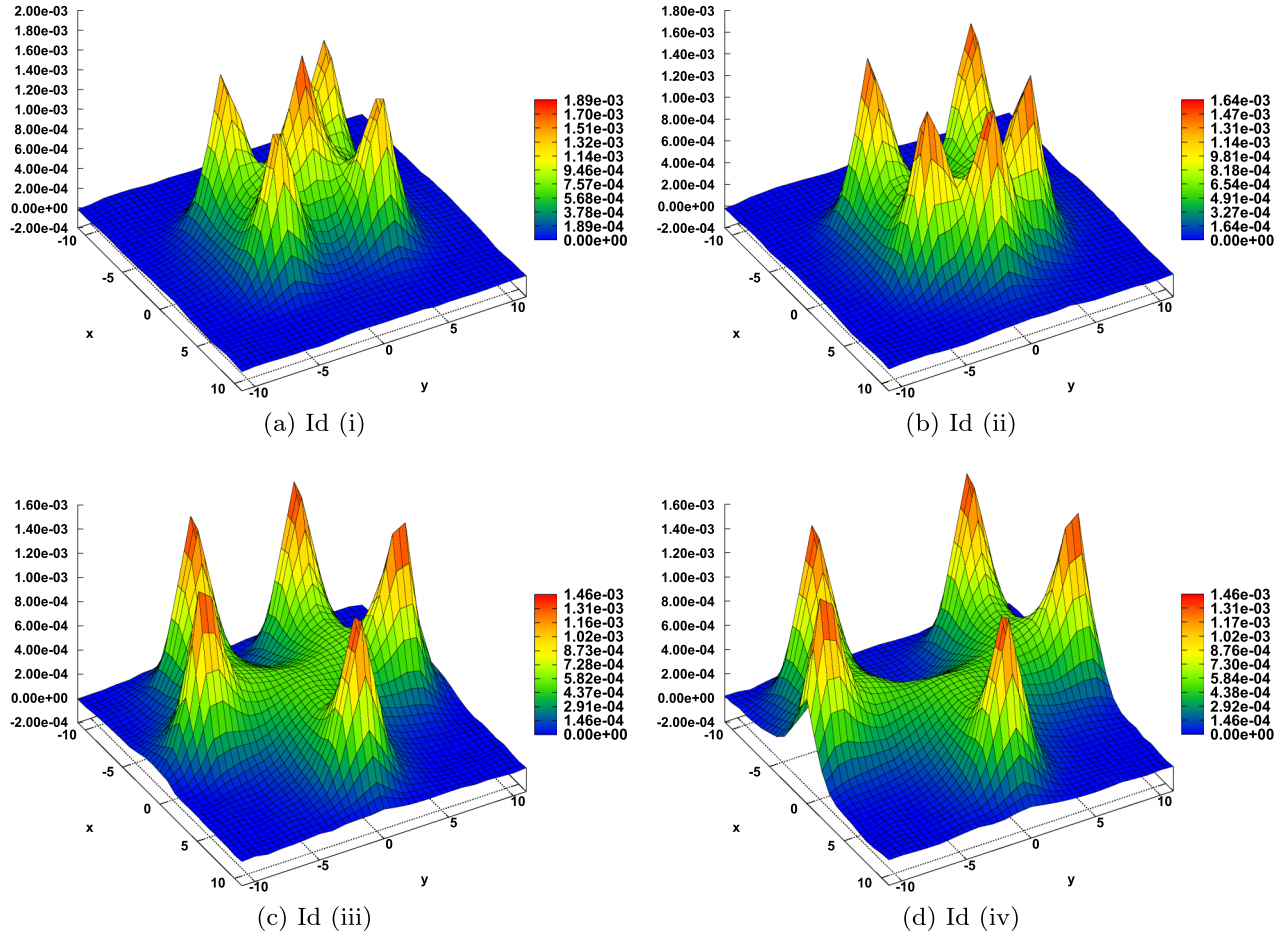

FIG. 5 (color online). We show three-dimensional plots of the Lagrangian density for the geometries defined in Table I. The density enhancement is maximal in the location of the color charges, and if the color charges were close the Coulomb potential would be important. With our geometries the color charges are separated, and the fundamental flux tubes connecting the charges and the Fermat-Steiner points are evident. The results are presented in lattice spacing units.

Cabibbo-Marinari pseudoheatbath and over-relaxation algorithm [40–42]. Our SU(3) updates involve three SU(2) subgroups, we work with nine complex numbers, and we reunitarize the matrix.

The results for the color fields, the energy and Lagrangian densities are shown in Figs. 4 and 5. The figures clearly exhibit multi-Y-type shaped flux tubes. We also plot the Fermat-Steiner points defined in Table II. The Fermat-Steiner points of geometries (i) and (ii) are of different type from the Fermat-Steiner points of geometries (iii) and (iv), since in the first geometries angles of 120° between the fundamental strings are not possible and thus the central Fermat-Steiner point has merged with the antiquark source. Nevertheless, and although the flux tubes have a finite width and are not infinitely thin as is assumed in the string flip-flop models, and although the Coulomb component of the potential is certainly important, we notice the junctions for the elementary flux tubes are clearly close to the computed Fermat-Steiner points. This validates the use of string flip-flop models for the quark confinement in constituent quark models.

TABLE II. Fermat-Steiner points for the pentaquark geometries studied. The geometry type is outlined in Fig. 3 and Table I.

	Fermat-Steiner points		
Id	$\mathbf{r}_I$	$\mathbf{r}_{II}$	$\mathbf{r}_{III}$
(i)	(0, −1.691, 0)	(0, 1.691, 0)	(0, 0, 0)
(ii)	(3.897, −3.830, 0)	(3.897, 3.830, 0)	(6, 0, 0)
(iii)	(−2.309, −4, 0)	(−2.309, 4, 0)	(0, 0, 0)
(iv)	(−2.309, −6, 0)	(−2.309, 6, 0)	(1.155, 0, 0)

In Fig. 6, we compare the chromoelectric field profile for the pentaquark, tetraquark, and the quark-antiquark system in the middle of the flux tube. The tetraquark and the quark-antiquark results were obtained by Ref. [35]. The three chromoelectric fields are identical up to the error bars. This confirms that the pentaquark flux tube is composed of a set of fundamental flux tubes with Fermat-Steiner junctions, and again validates the string flip-flop

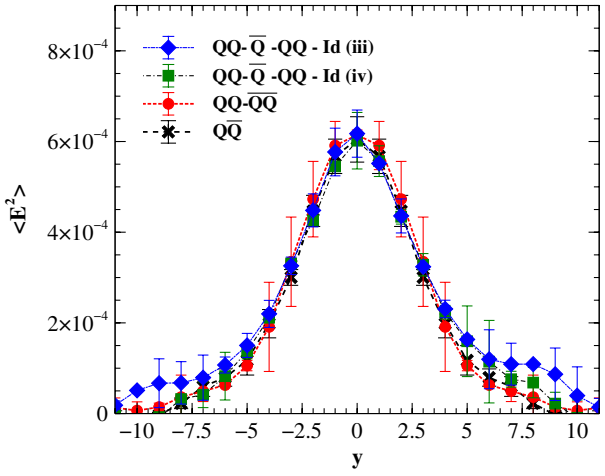

FIG. 6 (color online). Profile of the chromoelectric field for the pentaquark, tetraquark and quark-antiquark systems. The pentaquark profile corresponds to the geometry profile outlined in Fig. 3 and Table I along $x = 4$. The tetraquark and quark-antiquark results are from Ref. [35], in the middle of the flux tube.

models as models for the quark confinement in constituent quark models.

Multiquark stability is a subtle theoretical problem, requiring the correct understanding and calibration of the quark interactions. Combining our pentaquark results with the flux tube studies of mesons [43], baryons [44], hybrids [4], glueballs [45], and tetraquarks [35,36], we finally feel confident that the string flip-flop potential, where fundamental strings with the minimal possible length link the static color sources, is the correct phenomenological model for the confinement of any system of static quarks, antiquarks, and gluons. Whether the string flip-flop confining potential together with a correct short-range potential lead to multiquark narrow resonances or bound states remains a difficult quantum mechanical problem, but very interesting to the confinement and quark model experts.

Finally, as an outlook of the continuation of this work, to fully understand the pentaquark picture, namely the mixing between the pentaquark flux tube and the meson-baryon flux tube, it would be interesting to use the variational method as used in the tetraquark study done in Ref. [36].

ACKNOWLEDGMENTS

This work was partly funded by FCT Contracts No. POCI/FP/81933/2007, No. CERN/FP/83582/2008, No. PTDC/FIS/100968/2008, No. CERN/FP/109327/2009, No. CERN/FP/116383/2010, and No. CERN/FP/123612/2011. Nuno Cardoso is also supported by the FCT under Contract No. SFRH/BD/44416/2008.

[1] C. Alexandrou, P. de Forcrand, and O. Jahn, Nucl. Phys. B, Proc. Suppl. **119**, 667 (2003).
[2] H. Ichie, V. Bornyakov, T. Streuer, and G. Schierholz, Nucl. Phys. **A721**, 899 (2003).
[3] F. Okiharu and R. M. Woloshyn, Eur. Phys. J. C **35**, 537 (2004).
[4] M. Cardoso, N. Cardoso, and P. Bicudo, Phys. Rev. D **81**, 034504 (2010).
[5] N. Cardoso, M. Cardoso, and P. Bicudo, arXiv:1004.0166.
[6] I. J. General, P. Wang, S. R. Cotanch, and F. J. Llanes-Estrada, Phys. Lett. B **653**, 216 (2007).
[7] P. Bicudo and M. Cardoso, Phys. Rev. D **83**, 094010 (2011).
[8] J. Vijande, A. Valcarce, and J.-M. Richard, Phys. Rev. D **76**, 114013 (2007).
[9] P. Bicudo and M. Cardoso, Phys. Lett. B **674**, 98 (2009).
[10] J.-M. Richard, arXiv:0905.2308 [Acta Phys. Pol. (to be published)].
[11] M. W. Beinker, B. C. Metsch, and H. R. Petry, J. Phys. G **22**, 1151 (1996).
[12] S. Zouzou, B. Silvestre-Brac, C. Gignoux, and J. M. Richard, Z. Phys. C **30**, 457 (1986).
[13] B. A. Gelman and S. Nussinov, Phys. Lett. B **551**, 296 (2003).
[14] M. Karliner and H. J. Lipkin, Phys. Lett. B **575**, 249 (2003).
[15] A. De Rujula, H. Georgi, and S. Glashow, Phys. Rev. D **12**, 147 (1975).
[16] R. L. Jaffe, Phys. Rev. D **15**, 267 (1977).
[17] I. Adachi *et al.* (Belle Collaboration), arXiv:1105.4583.
[18] S. K. Choi *et al.* (Belle Collaboration), Phys. Rev. Lett. **91**, 262001 (2003).
[19] D. E. Acosta *et al.* (CDF II Collaboration), Phys. Rev. Lett. **93**, 072001 (2004).
[20] L. Maiani, F. Piccinini, A. D. Polosa, and V. Riquer, Phys. Rev. D **71**, 014028 (2005).
[21] S. Y. Jun *et al.* (SELEX Collaboration), prepared for Flavor Physics and *CP* Violation (FPCP 2004), Daegu, Korea, 2004.
[22] P. S. Cooper, J. Phys. Conf. Ser. **9**, 53 (2005).
[23] N. Mahajan, Phys. Lett. B **679**, 228 (2009).
[24] G. Cotugno, R. Faccini, A. D. Polosa, and C. Sabelli, Phys. Rev. Lett. **104**, 132005 (2010).
[25] A. Ali, C. Hambrock, and M. J. Aslam, Phys. Rev. Lett. **104**, 162001 (2010).
[26] A. V. Manohar, Nucl. Phys. **B248**, 19 (1984).
[27] M. Chemtob, Nucl. Phys. **B256**, 600 (1985).
[28] T. Nakano *et al.* (LEPS Collaboration), Phys. Rev. Lett. **91**, 012002 (2003).
[29] A. R. Dzierba, C. A. Meyer, and A. P. Szczepaniak, J. Phys. Conf. Ser. **9**, 192 (2005).
[30] A. M. Torres and E. Oset, Phys. Rev. Lett. **105**, 092001 (2010).
[31] C. Alexandrou, P. De Forcrand, and A. Tsapalis, Phys. Rev. D **65**, 054503 (2002).

[32] C. Alexandrou and G. Koutsou, Phys. Rev. D **71**, 014504 (2005).
[33] F. Okiharu, H. Suganuma, and T. T. Takahashi, Phys. Rev. D **72**, 014505 (2005).
[34] V. Bornyakov, P. Boyko, M. Chernodub, and M. Polikarpov, arXiv:hep-lat/0508006.
[35] N. Cardoso, M. Cardoso, and P. Bicudo, Phys. Rev. D **84**, 054508 (2011).
[36] M. Cardoso, N. Cardoso, and P. Bicudo, Phys. Rev. D **86**, 014503 (2012).
[37] F. Okiharu, H. Suganuma, and T. T. Takahashi, Phys. Rev. Lett. **94**, 192001 (2005).
[38] F. Okiharu *et al.*, arXiv:hep-ph/0507187.
[39] A. Hasenfratz and F. Knechtli, Phys. Rev. D **64**, 034504 (2001).
[40] N. Cardoso and P. Bicudo, J. Comput. Phys. **230**, 3998 (2011).
[41] N. Cardoso and P. Bicudo, Comput. Phys. Commun. **184**, 509 (2013).
[42] The CUDA codes are available at http://nemea.ist.utl.pt/~ptqcd.
[43] G. S. Bali, K. Schilling, and C. Schlichter, Phys. Rev. D **51**, 5165 (1995).
[44] T. T. Takahashi, H. Suganuma, and H. Ichie, arXiv:hep-lat/0401001.
[45] M. Cardoso and P. Bicudo, Phys. Rev. D **78**, 074508 (2008).